

**NPL REPORT MAT 17**

**The Effect of Heat Transfer  
Coefficients and Thermal  
Conductivity on Polymer  
Processing Simulation**

**ANGELA DAWSON,  
JEANNIE M. URQUHART  
and MARTIN RIDES**

**NOT RESTRICTED**

**MARCH 2008**



## **The Effect of Heat Transfer Coefficients and Thermal Conductivity on Polymer Processing Simulation**

A. Dawson, J. M. Urquhart and M. Rides  
Industry and Innovation Division

### **ABSTRACT**

The effects of heat transfer parameters key to industrial processing have been identified via polymer injection moulding process simulation. Moldflow finite element analysis software has been used to simulate injection moulding of components to investigate the relationship between injection moulding processing conditions and the effects of material properties on the moulding process. The effects of core and cavity side heat transfer coefficients, thermal conductivity and component thickness upon the injection moulding cycle time have been examined. Time to freeze for a moulding decreased with increasing polymer thermal conductivity, this effect becoming less pronounced with decreasing moulding thickness. Maximum injection pressure for a moulding increased with increasing polymer thermal conductivity with this effect becoming less pronounced with increasing moulding thickness. For a component, time to freeze decreased with increasing average heat transfer coefficient, although an effective lower limit to time to freeze was reached when core and cavity heat transfer coefficients values were set at 10,000 W/(m<sup>2</sup>.K) or above. These values for core and cavity heat transfer coefficients also set an effective upper limit for the maximum injection pressure for a component. Setting both core and cavity heat transfer coefficient values at 500 W/(m<sup>2</sup>.K) gave the lowest times to freeze and the lowest maximum injection pressures for all thicknesses. Setting the heat transfer coefficient values to 4,000 W/(m<sup>2</sup>.K) and 6,000 W/(m<sup>2</sup>.K) for core and cavity or cavity and core sides, respectively, produced the shortest time to freeze and highest maximum injection pressures of all the cases where the heat transfer coefficients were set at different values. The study has helped to improve understanding of the heat transfer taking place during injection moulding.

© Crown copyright 2008  
Reproduced with the permission of the Controller of HMSO  
and Queen's Printer for Scotland

ISSN 1754-2979

National Physical Laboratory  
Hampton Road, Teddington, Middlesex, TW11 0LW

Extracts from this report may be reproduced provided the source is acknowledged and  
the extract is not taken out of context.

Approved on behalf of the Managing Director, NPL,  
by Dr M G Cain, Knowledge Leader, Materials Team  
authorised by Director, Industry and Innovation Division

**CONTENTS**

<b>1</b>	<b>INTRODUCTION .....</b>	<b>1</b>
<b>2</b>	<b>COMPONENTS STUDIED .....</b>	<b>1</b>
<b>3</b>	<b>MATERIALS DATA .....</b>	<b>2</b>
<b>4</b>	<b>SIMULATIONS .....</b>	<b>2</b>
<b>5</b>	<b>RESULTS AND DISCUSSION .....</b>	<b>4</b>
<b>6.</b>	<b>UNCERTAINTIES .....</b>	<b>10</b>
<b>7</b>	<b>SUMMARY .....</b>	<b>12</b>
<b>8</b>	<b>REFERENCES.....</b>	<b>13</b>
<b>9</b>	<b>ACKNOWLEDGEMENTS .....</b>	<b>13</b>
	<b>APPENDIX A: UNCERTAINTY BUDGET FOR THERMOHAAKE THERMAL CONDUCTIVITY APPARATUS .....</b>	<b>14</b>
	<b>APPENDIX B: HEAT TRANSFER COEFFICIENT APPARATUS.....</b>	<b>16</b>



## 1 INTRODUCTION

The efficiency of polymer processing can be improved by reducing cycle times and reducing wastage of raw materials and energy. For polymers, heat transfer is crucial in determining cycle times due to their low thermal conductivity.

There are commercial and environmental drivers associated with reducing scrap rates, as well as the benefit of improving productivity through improved heat transfer. Warpage of products can occur due to excessive internal temperature gradients causing internal stresses, and degradation of polymer parts can occur through the formation of hot spots. Improving heat transfer could result in significant energy savings.

Heat transfer data can be utilised in modelling of the injection moulding process. The polymer part to be modelled by Finite Element Analysis (FEA) is represented as a mesh of discrete elements. The physical properties of the part are then attributed to these elements. For a physical event, a simulation is carried out and new physical properties of the object are then predicted that are caused by this event. FEA packages such as Moldflow® are available that specialise in polymer processing industry applications.

The relationships between injection moulding processing conditions and the effects of material properties on the moulding process have been investigated, using Moldflow Plastics Insight® (MPI), for simulating the injection moulding of polymer parts. The improved understanding of the heat transfer processes, during injection moulding gained from the modelling simulations can help companies reduce cycle times and improve conditions for polymer processing.

This report examines three key aspects in particular of polymer processing and part design:

1. effect of the mould core and mould cavity heat transfer coefficients
2. thermal conductivity of the polymer
3. thickness of the part being manufactured

## 2 COMPONENTS STUDIED

Circular discs 10 mm in diameter, of various thicknesses in the range 0.1 mm to 2 mm were studied. Experimental variables such as disc thickness, thermal conductivity of the polymer and mould core and mould cavity heat transfer coefficients were investigated using this simple geometric shape.

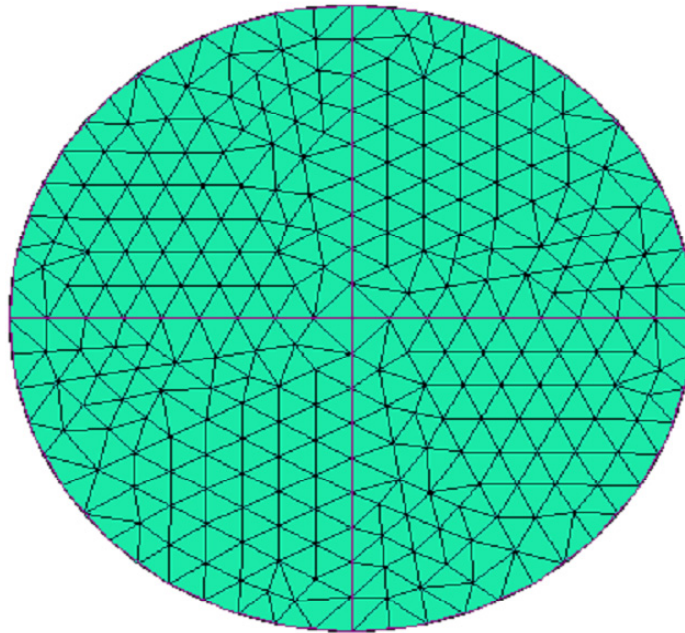


**Figure 1. Midplane mesh model of 10 mm disc.**

Figure 1 shows the model of the disc, modelled as a midplane mesh. The injection location is the central point with injection direction normal to the midplane. A cooling circuit was produced for this model using MPI, to simulate cooling with water at 20°C.

### **3 MATERIALS DATA**

Material properties data for the commercial grade (Solvay Eltex TUB121) of high-density polyethylene and for the mould material (Tool Steel-P20 used for this study) were taken from the suppliers' datasheets. Measurements were made of the HDPE's thermal conductivity using a line source probe method. The initial value of thermal conductivity used in the modelling study for was taken to be the measured value of 0.247 W/(m.K).

### **4 SIMULATIONS**

A fill-cool-flow process sequence was used for analysis using the Moldflow® simulations and analysis. The default automatic filling control and automatic velocity/pressure switch over were used for the simulations. The injection moulding parameters applied to the simulations are listed in Table 1. The default packing profile was selected. The injection time, cooling time and the velocity/pressure switch-over being determined automatically.

**Table 1: Injection moulding parameters applied to simulations**

<b>Injection moulding parameter</b>	<b>Set value for simulation</b>
Maximum machine clamp force, tonnes	7000
Maximum injection pressure, MPa	180
Maximum machine injection rate, cm <sup>3</sup> /s	5000
Maximum hydraulic response time, s	0.01
Packing/holding time, s	10
Cavity-side mould surface temperature, °C	35
Core-side mould surface temperature, °C	35
Melt temperature, °C	255
Ambient temperature, °C	25

The ‘time to freeze part’ ( $T_f$ ) result is defined by Moldflow as ‘the amount of time taken for all the elements in the part to freeze to the ejection temperature, measured from the start of the cycle’. The disc analyses used the Moldflow recommended ejection temperature for this polymer, that is 90°C.

Three simulations were carried out to look at the effects of:

1. Symmetrically and asymmetrically applied heat transfer coefficients on different thickness discs of 10 mm diameter HDPE of thermal conductivity 0.247 W/(m.K).
2. Asymmetrically applied heat transfer coefficients totalling 10,000 W/(m<sup>2</sup> K) on different thickness discs of 10 mm diameter HDPE of thermal conductivity 0.247 W/(m.K).
3. Thermal conductivities of 0.247 W/(m.K), 0.247 W/(m.K) ± 15%, and 0.247 W/(m.K) ± 50% applied to different thickness 10 mm diameter HDPE discs with heat transfer coefficients set at 1,000 W/(m<sup>2</sup>.K) and 10,000 W/(m<sup>2</sup>.K).

## 5 RESULTS AND DISCUSSION

### 5.1 THE EFFECT OF VARYING THE CAVITY (SPRUE SIDE) AND CORE SIDE MOULD-MELT HEAT TRANSFER COEFFICIENTS ON TIME TO FREEZE AND MAXIMUM INJECTION PRESSURE

Initially, for simulation 1, a range of asymmetric and symmetric cavity and core side mould melt heat transfer coefficients were selected and the effect on time to freeze was investigated (Figures 2 and 3).

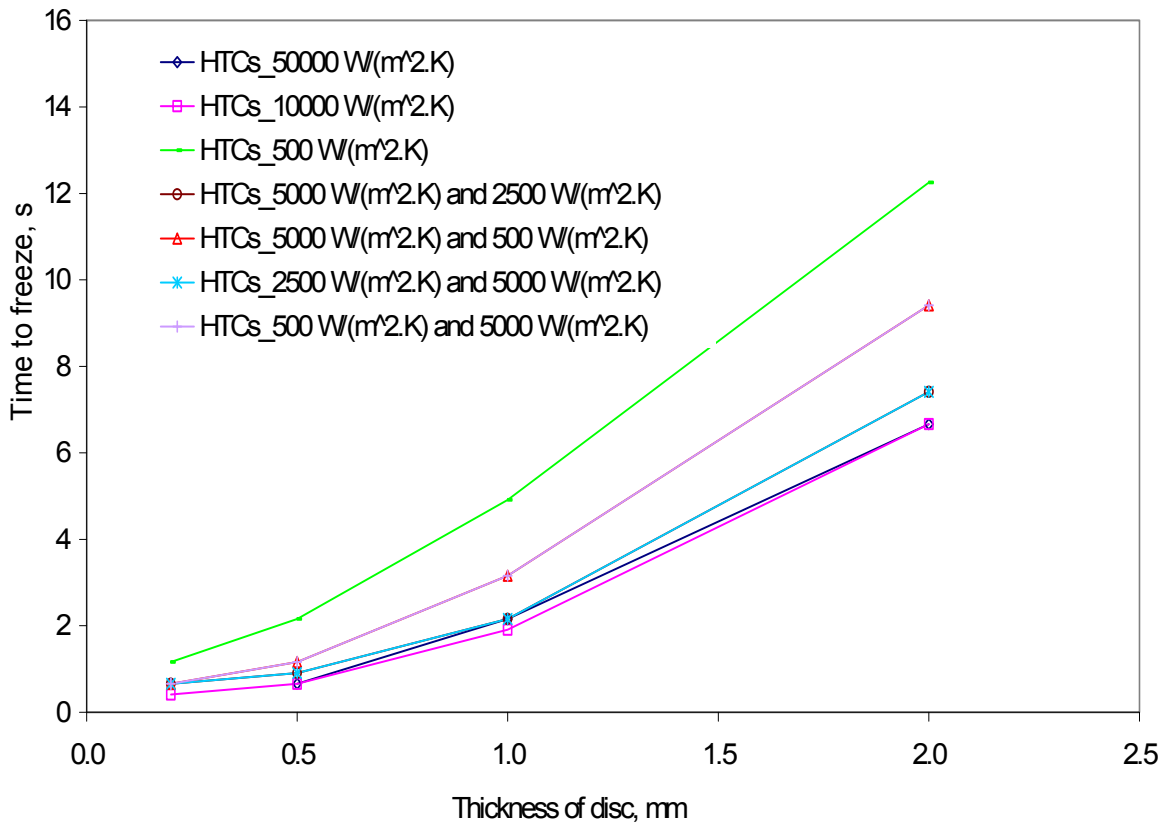


**Figure 2. Effect of asymmetric and symmetric values of core and cavity heat transfer coefficients on time to freeze for 10 mm diameter discs of varying thicknesses.**

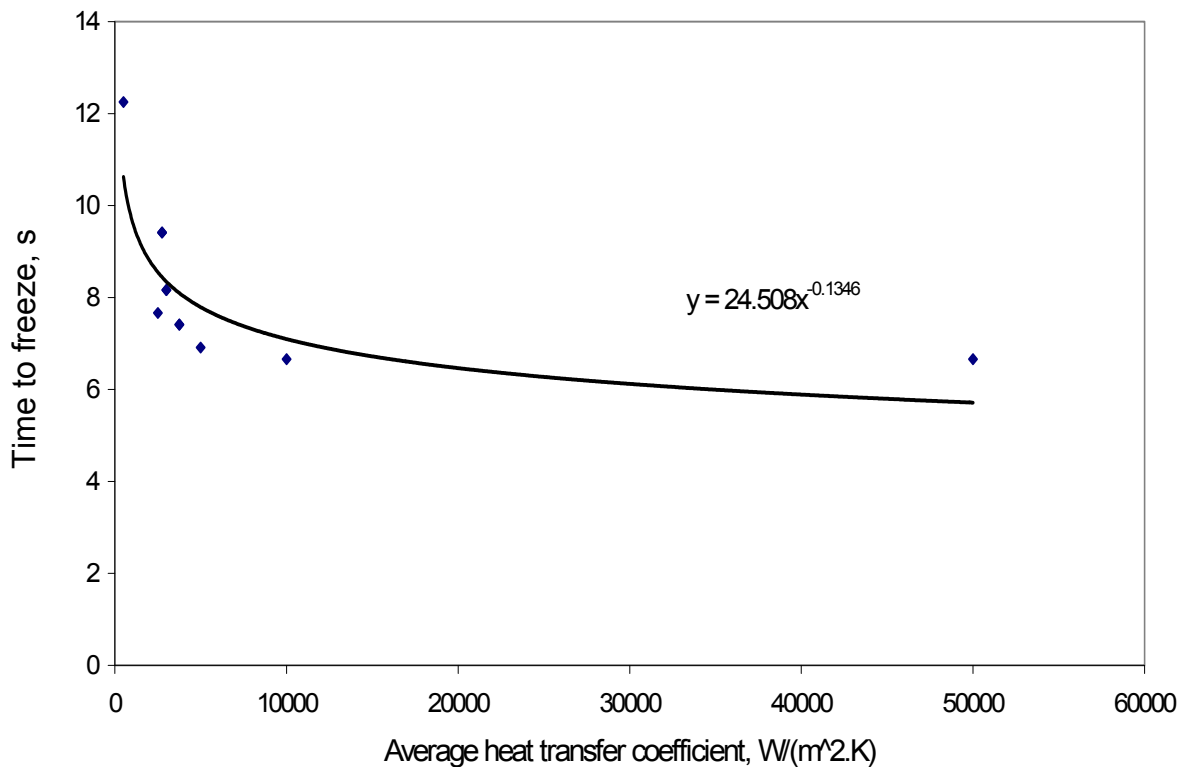


**Figure 3. Effect of average of symmetric and asymmetric core and cavity heat transfer coefficients on time to freeze for a 2 mm thick 10 mm diameter disc.**

Time to freeze decreased with decreasing thickness of the disc (Figure 2) for all configurations of core and cavity side heat transfer coefficients. The fastest time to freeze for discs of all thicknesses was given by the two symmetric configurations where the values of core and cavity heat transfer coefficients were 50,000  $W/(m^2.K)$  and 10,000  $W/(m^2.K)$ . The slowest time to freeze for discs of all thicknesses was given by the symmetric configuration where the core and cavity heat transfer coefficients were both 500  $W/(m^2.K)$ .

The asymmetric configurations, where initially the core and cavity heat transfer coefficients were set at 5,000  $W/(m^2.K)$  and 2,500  $W/(m^2.K)$  respectively, and then with these heat transfer coefficient values reversed, produced the same time to freeze for each configuration demonstrating the symmetry of the disc model selected. The same reversibility was observed when heat transfer coefficients of 5,000  $W/(m^2.K)$  and 500  $W/(m^2.K)$  were used.

For a disc of constant thickness (2 mm), the time to freeze, tended to decrease with the increasing average of the core and cavity heat transfer coefficients (Figure 3). For average heat transfer coefficient values of 10,000  $W/(m^2.K)$  and above, the time to freeze reached a constant value.

The effect of the different cavity and core heat transfer coefficients on maximum injection pressure was investigated for the range of asymmetric and symmetric cavity and core side mould-melt heat transfer coefficients previously selected (Figures 4 and 5). The maximum injection pressure increased with decreasing thickness of disc (Figure 4) for all configurations of core and cavity side heat transfer coefficients. The highest maximum injection pressure for discs of all thicknesses was given by the two symmetric configurations where the values of core and cavity heat transfer coefficients were 50,000 W/(m<sup>2</sup>.K) and 10,000 W/(m<sup>2</sup>.K). The lowest maximum injection pressure for discs of all thicknesses was given by the symmetric configuration where the core and cavity heat transfer coefficients were both 500 W/(m<sup>2</sup>.K) (the lowest value used).

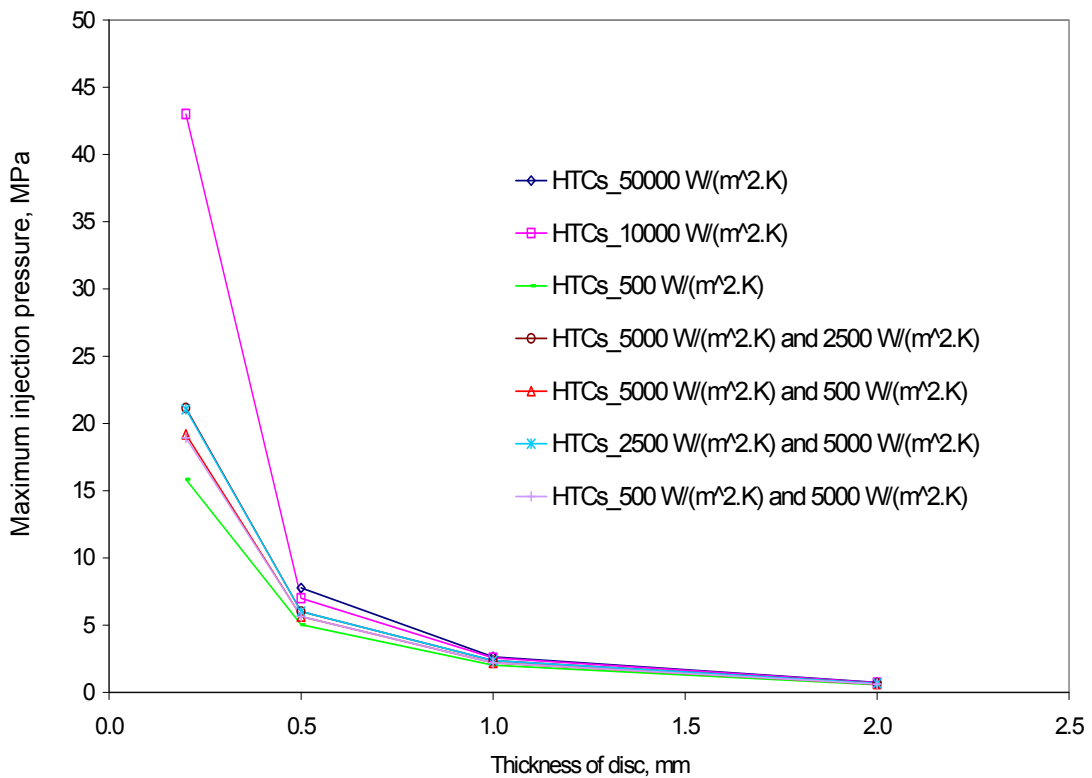


**Figure 4. Effect of asymmetric and symmetric values of core and cavity heat transfer coefficients on maximum injection pressure for 10 mm diameter discs of varying thicknesses.**

The asymmetric configurations where initially the core and cavity heat transfer coefficients were set at 5,000 W/(m<sup>2</sup>.K) and 2,500 W/(m<sup>2</sup>.K) respectively, and then with these heat transfer coefficient values reversed, produced the same maximum injection pressure for each configuration demonstrating the symmetry of the disc model selected. The same reversibility of core and cavity heat transfer coefficients was observed for the asymmetric configuration where heat transfer coefficients of 5,000 W/(m<sup>2</sup>.K) and 500 W/(m<sup>2</sup>.K) were used.

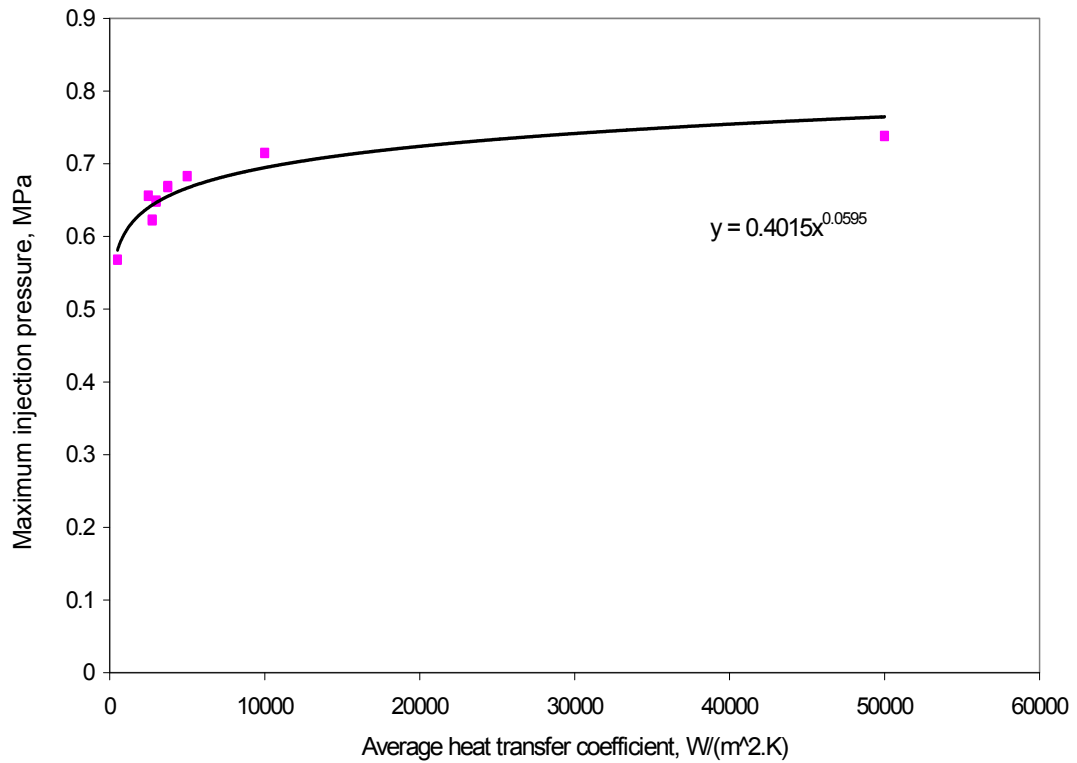


**Figure 5. Effect of average of symmetric and asymmetric core and cavity heat transfer coefficients on maximum injection pressure for a 2 mm thickness, 10 mm diameter disc.**

For a disc of constant thickness (2 mm), the maximum injection pressure for the part increased with the increasing average of the core and cavity heat transfer coefficients (Figure 5). For average heat transfer coefficient values of 10,000 W/(m<sup>2</sup>.K) and above the maximum injection pressure reached a constant value.

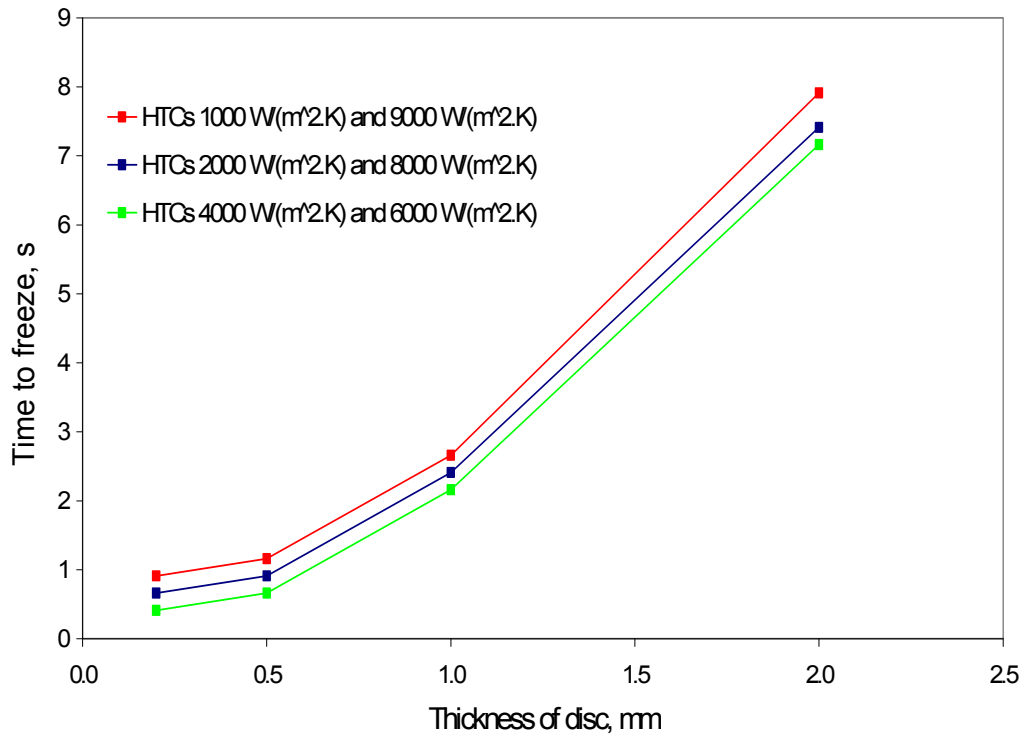


**Figure 6. Effect of asymmetric values of core and cavity heat transfer coefficients totalling  $10,000 \text{ W}/(\text{m}^2 \cdot \text{K})$  on time to freeze for 10 mm diameter discs of varying thicknesses.**

For simulation 2, a range of asymmetric cavity and core side mould-melt heat transfer coefficients were selected to give a totalled heat transfer coefficient value of  $10,000 \text{ W}/(\text{m}^2 \cdot \text{K})$  when the cavity and core side heat transfer coefficients were added together (Figure 6).

The time to freeze decreased with decreasing thickness of the disc, for all three simulated cases (Figure 6.). The longest time to freeze values were obtained for the case where the HTC was largest on one side of the mould and smallest on the other side for all disc thicknesses. The shortest time to freeze values were observed for the case where the core and cavity mould-melt HTC values were similar at  $6,000 \text{ W}/(\text{m}^2 \cdot \text{K})$  and  $4,000 \text{ W}/(\text{m}^2 \cdot \text{K})$ .

## 5.2 THE EFFECT OF VARYING THE HDPE THERMAL CONDUCTIVITY AND THE DISC THICKNESS

For simulation 3, 10 mm diameter discs of four thicknesses (2 mm, 1 mm, 0.5 mm and 0.2 mm) and of thermal conductivities ( $0.247 \text{ W}/(\text{m} \cdot \text{K})$ ,  $0.247 \text{ W}/(\text{m} \cdot \text{K}) \pm 15\%$ , and  $0.247 \text{ W}/(\text{m} \cdot \text{K}) \pm 50\%$ ) were modelled (Figures 7 and 8). The cavity side mould-melt HTC value of  $1,000 \text{ W}/(\text{m}^2 \cdot \text{K})$  and the core side mould-melt HTC value of  $10,000 \text{ W}/(\text{m}^2 \cdot \text{K})$  were kept constant for all cases.

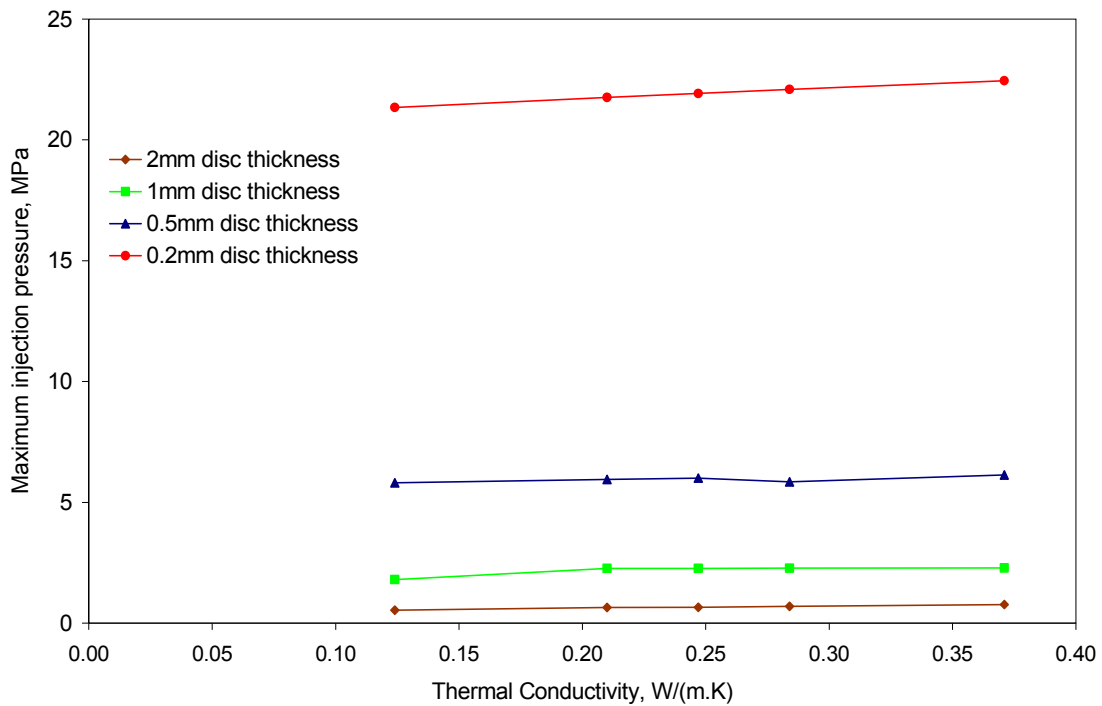


**Figure 7. The effect of varying thermal conductivity of HDPE on the maximum injection pressure of moulded discs of different thicknesses.**

For discs of all thicknesses, the maximum injection pressure increased with increasing thermal conductivity. This observed effect was greater for the thinnest section parts. The highest maximum injection pressures were achieved during the moulding of the thinnest disc, and the lowest maximum injection pressures were observed during the production of the thickest disc.

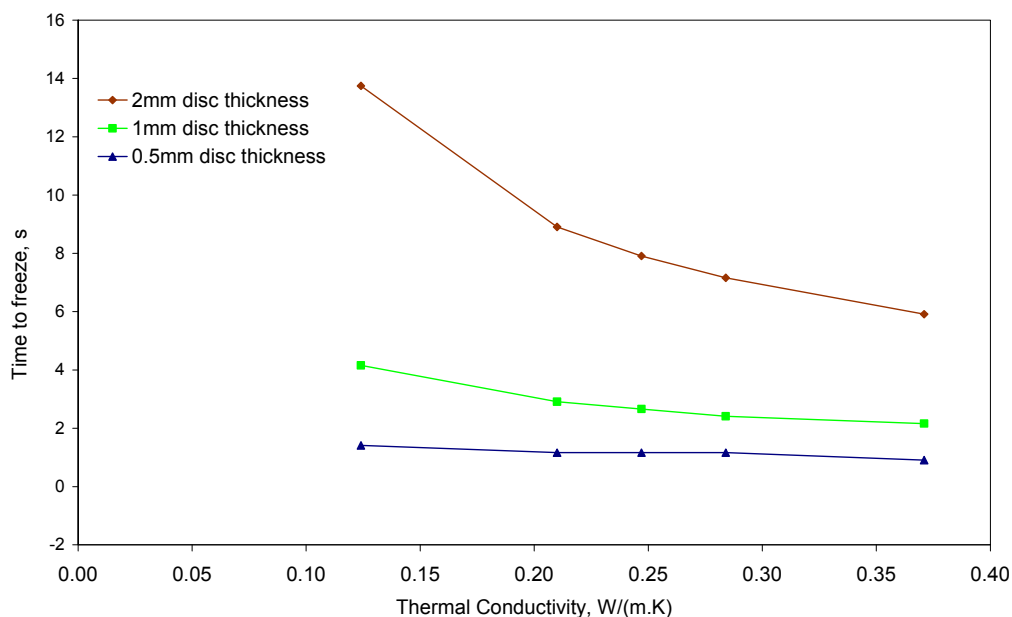


**Figure 8. The effect of varying thermal conductivity of HDPE on the time to freeze of moulded discs of different thicknesses.**

Time to freeze decreased with decreasing disc thickness for 2 mm, 1 mm and 0.5 mm discs. Time to freeze decreased with increasing thermal conductivity of HDPE and this effect was greatest for the thickest disc, the 2 mm thickness disc.

## 6. UNCERTAINTIES

An uncertainty budget for the thermal conductivity line source probe apparatus has been included (Appendix A). The overall uncertainty for this technique was calculated to be 20.7%, with a contribution coming from the repeatability at ambient pressure calculated as 15.6%. At 160 MPa pressure, the repeatability of the line source probe was calculated as 8.0%. This compares with a repeatability for a heat flow meter of 3.0% [1] and the repeatability of 3%-6% quoted for the standard test method for a transient line-source technique [2].

An intercomparison of thermal conductivity and thermal diffusivity measurement techniques (temperature wave analysis, laser flash, transient plane source (Hot Disk), transient line-source probe, and heat flux meter methods) demonstrated that there was very good agreement of both thermal conductivity and thermal diffusivity results, with values being within a range of approximately  $\pm 7\%$  and  $\pm 9\%$  respectively [1]. Furthermore, there was similar good agreement between thermal conductivity and thermal diffusivity values, when thermal conductivity values were converted to thermal diffusivity values (and vice-versa) using specific heat capacity and density data. Typically, the values were within a range of approximately  $\pm 10\%$ .

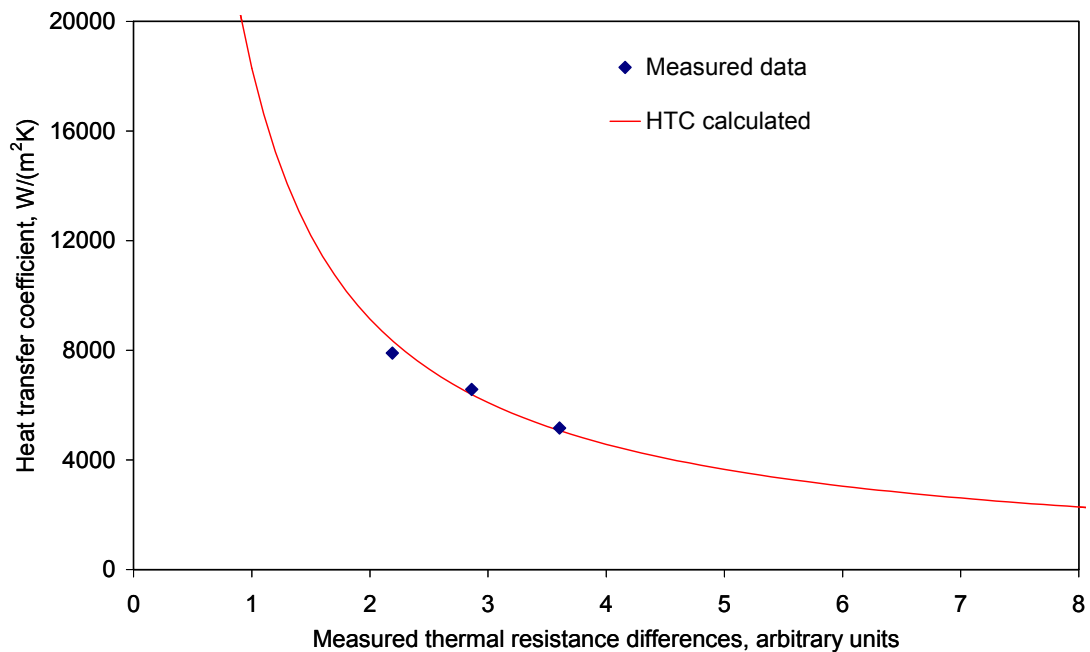


**Figure 9: Effect of errors on derived heat transfer coefficients**

For HTC coefficient measurements (Appendix B) the uncertainty in measured values was considered to be high. The measurement method is based on the determination of small differences between large values. Actual experimental results have been

superimposed on the plot (Figure 9). This clearly indicates that very large values in HTC can be erroneously obtained, but that excessively low values are more unlikely. The results can therefore be considered to represent a reasonable lower limit to HTC values with greater confidence, whereas as an upper limit value there is considerably more uncertainty in the values. This is based on the observation that an error in the increasing x-direction from the ‘true’ value has a smaller effect on the derived HTC value compared with an equivalent error in the decreasing x-direction, (Figure 9). Large errors resulting in negative abscissa values would result in negative HTC values being obtained, again with an asymptotic form, increasing in magnitude when approaching  $x = 0$ . Some such results were obtained in the testing performed, indicating the magnitude of the errors. Statistical analysis of all the tests to determine the lower limit of the mean of the heat transfer coefficient at a 95% confidence level (2 standard deviations of the standard error) yielded a value of approximately 4700 W/(m<sup>2</sup> K) (thermal contact resistance of  $\approx 0.0002$  m<sup>2</sup> K/W), but no sensible upper limit to the heat transfer coefficient value could be stated with any degree of confidence.

**Table 2. Effect of changes in thermal conductivity value on time to freeze and maximum injection pressure values for 10 mm disc**

Disc thickness, mm	% Change in thermal conductivity from measured value of 0.247 W/(m.K)	% Change of time to freeze compared with that obtained using the measured value of thermal conductivity	% Change of maximum injection pressure, MPa compared with that obtained using measured value of thermal conductivity
2	- 50	+73.8	-18.1
2	- 15	+12.6	-0.6
2	0	0	0
2	+15	-9.5	6.23
2	+50	-25.2	17.3
1	- 50	+56.4	-20.5
1	- 15	+9.4	0
1	0	0	0
1	+15	-9.4	0.2
1	+50	-18.8	0.5
0.5	- 50	+21.6	-3.2
0.5	- 15	0	-0.9
0.5	0	0	0
0.5	+15	0	-2.5
0.5	+50	-21.6	2.13
0.2	- 50	+54.9	-
0.2	- 15	+54.9	-
0.2	0	0	-
0.2	+15	0	-
0.2	+50	-77.5	-

The effect of a 50% uncertainty in the thermal conductivity measured value on time to freeze was greatest for the thinnest disc, 0.2 mm thick. When the thermal conductivity value was decreased by 50% and 15%, a 54.9% increase in time to freeze was observed

for both cases for the 0.2 mm thick disc. When the thermal conductivity value was increased by 50%, a 77.5% decrease in time to freeze was observed.

The effect of a 50% uncertainty in the thermal conductivity value on maximum injection pressure was greatest for the two thickest discs (1 mm and 2 mm). A decrease of 50% in the thermal conductivity value led to a predicted decrease of 18.1% in maximum injection pressure for the 2 mm disc and a decrease of 20.5% in maximum injection pressure for the 1 mm disc.

The effect of uncertainties in HTC were investigated by taking a HTC value of 5000 W/(m<sup>2</sup>.K) as a nominal experimental HTC value and comparing the time to freeze and maximum injection pressures predicted for this HTC value with these values predicted for the average HTC values used in simulation 1 (Table 3).

**Table 3. Effect of changes in HTC on time to freeze and maximum injection pressure for 10 mm disc**

<b>Average HTC, W/(m<sup>2</sup>.K)</b>	<b>% Change in average HTC compared with average HTC value of 5000 W/(m<sup>2</sup>.K)</b>	<b>% Change in time to freeze compared with time to freeze predicted for 5000 W/(m<sup>2</sup>.K) HTC value</b>	<b>% Change in maximum injection pressure compared with maximum predicted for 5000 W/(m<sup>2</sup>.K) HTC value</b>
50000	900	-3.6	8.1
10000	100	-3.6	4.6
5000	0	0	0
2500	-50	10.9	-4.0
500	-90	77.3	-16.8
3750	-25	7.2	-2.0
3000	-40	18.1	-5.0
2750	-45	36.2	-8.8
3750	-25	7.2	-2.2
3000	-40	18.1	-5.2
2750	-45	36.2	-8.9

The greatest increase in time to freeze (77.3%) was predicted for a 90 % decrease in average HTC value. Small decreases (3.6%) in time to freeze were predicted for 100% and 900% increases in average HTC values. A 50% decrease in the average HTC value brought about a 10.9% increase in time to freeze (Table 3).

The greatest decrease in maximum injection pressure (16.8%) was predicted for a 90% decrease in average HTC value. An 8.1% increase in maximum injection pressure was predicted for a 900% increase in average HTC value compared with an 8.8% decrease in maximum injection pressure predicted for a 45% decrease in HTC value.

## 7 SUMMARY

The thermal conductivity of the polymer melt is a dominant heat transfer parameter in the injection moulding process. Time to freeze decreased as the thermal conductivity increased for a part of constant thickness, whereas maximum injection pressure for that

part increased as the thermal conductivity of the material used to mould the part was increased.

In all cases the time to freeze decreased as the thickness of the part decreased and the inverse relationship was true of maximum injection pressure and thickness.

The fastest time to freeze for thin walled discs was simulated for symmetrical core and cavity mould-melt HTC values of 10,000 W/(m<sup>2</sup>.K) and 50,000 W/(m<sup>2</sup>.K). These conditions would be hard to achieve in practice. The fastest time to freeze was achieved for asymmetric core and cavity HTC values of 4,000 W/(m<sup>2</sup>/K) and 6,000 W/(m<sup>2</sup>.K).

Uncertainties in thermal conductivity were most significant for thin walled parts. The greater the uncertainty in the thermal conductivity measurement the greater the effect on time to freeze and maximum injection pressure predicted values.

Uncertainties in HTC values appear to be have more significance for low HTC values than for high HTC values.

## **8 REFERENCES**

- 1 M. Rides, J. Morikawa, L. Halldahl, B. Hay, H. Lobo, A. Dawson, C. Allen, Intercomparison of thermal conductivity and thermal diffusivity methods for plastics, to be published.
- 2 ASTM D5930 Standard Test Method For Thermal Conductivity of Plastics By Means of a Transient Line-Source Probe Technique.

## **9 ACKNOWLEDGEMENTS**

This work was carried out as part of a programme of underpinning research sponsored by the National Measurement System Directorate of the Department for Innovation, Universities and Skills, UK. The authors would like to thank Eric Henry (Moldflow Ltd.) and Moldflow Ltd. for provision of the Moldflow Plastics Insight software. The advice, guidance and contributions from members of the Polymeric Materials Industrial Advisory Group are gratefully acknowledged.

## **APPENDIX A: UNCERTAINTY BUDGET FOR THERMOHAAKE THERMAL CONDUCTIVITY APPARATUS**

### **1 Sources of Uncertainty**

#### **Type A Uncertainties**

##### **1.1 Repeatability**

The repeatability of the thermal conductivity values for ten samples of PDMS NDJ200 on cooling from 110°C to 30°C at atmospheric pressure was calculated as  $\pm 1.4\%$  at the 95% confidence level. The repeatability of the thermal conductivity values for ten samples of HDPE HCE000 on cooling from 170°C to 50°C at atmospheric pressure was calculated at  $\pm 15.6\%$  at the 95% confidence level.

##### **1.2 Reproducibility**

The repeatability of the thermal conductivity values for five samples of HDPE HCE000 on cooling from 170°C to 50°C at atmospheric pressure was calculated for operator 1 and found to be  $\pm 14.6\%$  at the 95% confidence level. A second operator repeated the tests on a further five samples of HDPE HCE000 under the same test conditions. The repeatability for operator 2 was calculated to be  $\pm 8.8\%$  at the 95% confidence level. The results from the two operators were pooled and an overall reproducibility for the thermal conductivity values was calculated to be  $\pm 13.6\%$  at the 95% confidence level.

#### **Type B Uncertainties**

##### **1.3 Non-uniformity of Heat Input**

The voltage across the heating wire resistor within the thermal conductivity probe can vary by a maximum of  $\pm 5\text{mV}$ . This is a 0.002% change in the standard voltage of 2.5V applied during the test procedure which in turn, from the mathematical relationship between heat input and thermal conductivity, equates to a thermal conductivity uncertainty of  $\pm 0.002\%$ .

##### **1.4 Effect of Change In Sample Length**

The sample mass of the sample was varied to give an average sample length of 50mm for five samples and an average sample length of 70mm for another five samples. There was an average difference of 0.00097% between the mean thermal conductivity values for the two sample lengths across the temperature range of measurement of HDPE HCE000, which is not a significant difference. Therefore within the limits of these two sample lengths, the sample length variation has no effect on the overall thermal conductivity uncertainty and can be ignored.

##### **1.5 Non-uniformity of Temperature**

The temperature measured within the thermal conductivity probe and at the wall of the sample cell can vary by  $\pm 0.3^\circ\text{C}$  over a 120°C temperature range. As the calculation of thermal conductivity depends on the temperature change that occurs within the sample and not the absolute temperature, when a 30 second pulse of heat energy is applied to the sample, then the error is assumed to be a systematic error only and can be ignored.

### 1.6 Computer Timebase

The uncertainty in the measurement of time associated with the computer clock is  $\pm 3$  seconds within 24 hours, which is a percentage uncertainty of 0.0035%. As this uncertainty is very small in comparison to the final overall uncertainty it can be ignored

## 2 Uncertainty Budget Table

	Value $\pm$ %	Probability Distribution	Divisor	$C_i$	Uncertainty Contribution $\pm$ %	Uncertainty Squared $\pm$ %	$V_i$ or $V_{eff}$
<b>Type A</b>							
Repeatability	15.6@ 2 std devs	Normal	2	1	7.815 @ 1 std dev	61.07	89
Reproducibility	13.6@ 2 std devs	Normal	2	1	6.801 @ 1 std dev	46.25	89
<b>Type B</b>							
Non- uniformity of heat input	0.002	Rectangular	1.73	1	0.00116	1.34E-06	$\infty$
Non-uniformity of temperature	0.0	Rectangular	1.73	1	0.000	0.000	$\infty$
Sample height	0.0	Rectangular	1.73	1	0.000	0.000	$\infty$
Time	0.0	Normal	1	1	0.000	0.000	$\infty$
					<b>Calculation of Uncertainty</b>		
					<b>Sum of squares</b>	107.3 %	
					<b>Square root of sum of squares</b>	10.4 %	
					<b>Multiplication by k= 2 for 95% confidence level</b>	<b><math>\pm 20.7\%</math> Final Uncertainty Value</b>	

## APPENDIX B: HEAT TRANSFER COEFFICIENT APPARATUS

Method for determining the heat transfer coefficient across an interface.

The apparatus consisted of two parallel, circular steel plates sandwiching the polymer specimen, which was in the form of a thin disc of the same diameter as the plates, Figure 1. The bottom ‘hot’ plate was temperature controlled using circular electric heaters. The top ‘cold’ plate acted as a heat sink. Thus the heat flow was from the bottom plate to top plate. Heat flux sensors (Micro-Foil™ Heat Flux Sensors type 20457-1, RdF Corporation) and thermocouples were located in both the upper and lower plates and were logged simultaneously using a Labview® data logging system. The heat flux sensor provides a voltage output proportional to the heat flux. However, a third order polynomial was used to correct for its temperature dependence. The vertical position of the upper plate could be adjusted to allow for various specimen thicknesses and to enable repeatable thermal contact with the specimen to be achieved.

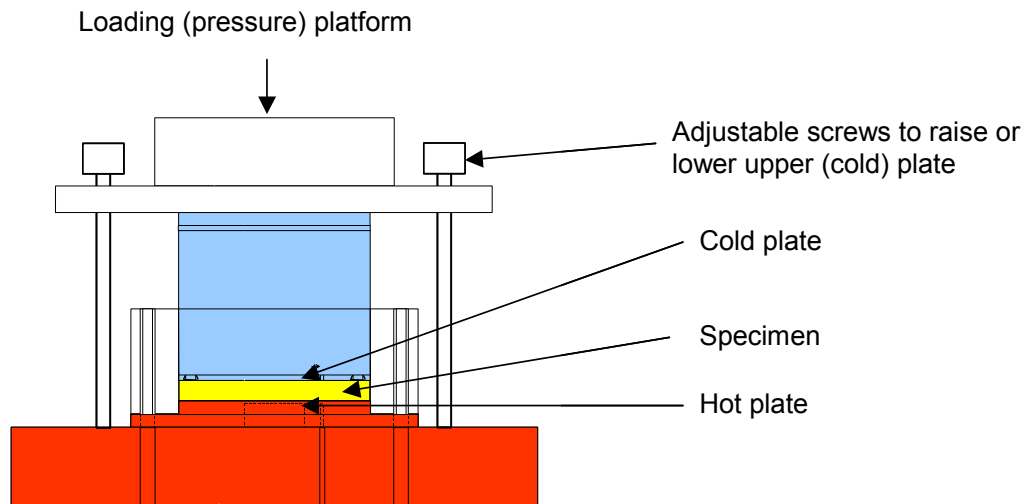


**Figure 1: Heat transfer coefficient apparatus.**

Test specimens were produced from polymer granules by compression moulding and left to cool slowly to room temperature under pressure to minimise residual stresses and distortion. The thicknesses of the specimens were measured prior to testing using a hand-held micrometer and also in situ during testing using a laser micrometer system.

The concept of thermal resistances has been used to analyse the raw data and determine the heat transfer properties of the specimens and interfaces tested using the HTC instrument - see Section 3.

By placing the top and bottom plates in contact with each other, and with the instrument set to the test temperature, the baseline thermal resistance  $R_{inst}$  for the instrument was determined by measuring the temperatures of the top and bottom plates and the heat flux through the sensor in the bottom plate. This baseline thermal resistance accounted for interface heat transfer coefficients and plate thermal conductivities within the instrument and was used to correct subsequent data. The test specimen was then inserted between the ‘hot’ and ‘cold’ plates and again thermal equilibrium was attained

before temperature and heat flux readings were taken to determine the thermal resistance of the experimental arrangement with specimen. To reach thermal equilibrium the apparatus was left for at least 6 hours. Steady state conditions were assessed by examining the constancy of the temperature and heat flux signals.

The instrument was calibrated by comparing the measured value of thermal conductivity for a reference PMMA material with its known thermal conductivity [13], determined using a guarded hot plate instrument. Thus the heat transfer coefficient instrument reported here is a comparative rather than absolute method.

The concept of thermal resistances  $R$  ( $\text{m}^2\cdot\text{K}/\text{W}$ ) is invaluable for studying the thermal behaviour of a series of elements (layers) with interfaces, the elements being represented by their thermal conductivity and the interfaces by their heat transfer coefficient. The total thermal resistance of the layered structure,  $R$ , is given by the sum of the thermal resistances,  $r_i$ , of all the elements and interfaces<sup>1</sup>. The thermal resistance of an element or interface is given by:

$$r = \frac{\delta T}{q} \quad (1)$$

where  $\delta T$  is the temperature difference and  $q$  the heat flux. For a specimen of thickness  $x$ , with temperatures  $T_h$  and  $T_c$  at the bottom (hot) and top (cold) surfaces respectively, and heat flux  $q$  ( $\text{W}/\text{m}^2$ ) through the specimen, the thermal conductivity  $\lambda$  ( $\text{W}/(\text{m}\cdot\text{K})$ ) is given by:

$$\lambda = \frac{q x}{T_h - T_c} \quad (2)$$

Similarly, the heat transfer coefficient  $h$ ,  $\text{W}/(\text{m}^2\cdot\text{K})$  at the interface of two surfaces in contact is given by:

$$h = \frac{q}{T_h - T_c} \quad (3)$$

where  $T_h$  is the temperature at the ‘hot’ interface side and  $T_c$  is the temperature at the ‘cold’ interface side. For a element (layer) of thickness  $x_l$  then using Equations 1 and 2:

$$r_l = \frac{\delta T}{q} = \frac{x_l}{\lambda_l} \quad (4)$$

and for an interface with heat transfer coefficient  $h_i$  using Equations 1 and 3:

$$r_i = \frac{\delta T}{q} = \frac{1}{h_i} \quad (5)$$

Thus the total thermal resistance of a layered structure of elements and interfaces can be expressed as:

---

<sup>1</sup> From this point on, an upper case  $R$  is used to denote directly measurable quantities (using Equation 7) whereas lower case  $r$  is used to denote component thermal resistances.

$$R = \sum r = \sum_l \frac{x_l}{\lambda_l} + \sum_i \frac{1}{h_i} \quad (6)$$

where  $h_i$  is the heat transfer coefficient of the  $i^{\text{th}}$  interface, and  $\lambda_l$  the thermal conductivity of the  $l^{\text{th}}$  layer of thickness  $x_l$ .

For the instrument the measured thermal resistance  $R_i$  is given by

$$R = \frac{T_h - T_c}{q} \quad (7)$$

where  $T_h$  is the lower ‘hot’ plate temperature,  $T_c$  is the upper ‘cold’ plate temperature and  $q$  is the heat flux.